Detection and Classification of Circular Structures on Spot Images

Jean-François Parrot and Hind Taud

Abstract—**The unsupervised method proposed here for detecting structural features on satellite images consists of three major steps:**

a. **The extraction of contours, which depends on the encountered texture, is obtained by an iterative filtering followed by several thresholds that generate binary images. The thresholds are determined by different percentages of pixels over the total number of pixels contained in the image. We then trace the limits of the binary forms previously filtered by an iterative majority smoothing.**
b. **The detection of the structures from the contours involves four substeps: individualization of the curves; decomposition of the curves into subcircular elements; application of a version of the Hough transform to each subcircular elements; computation of precise results.**
c. **The computation of parameters that discriminate the detected structures; namely, for each structure, the position of the center and radius of the reference circle, the number of detected pixels, the chord and the intersection coefficients, the normal direction and the distance between the middle of the chord, and the intersection point between normal and chord. This set of data allows us to select the different families of structures that we are looking for.**

As an example, the method has been applied to the region of Azru, which presents on both geological and geomorphological levels, numerous circular structures of varied origins.

I. Introduction

THE automated detection of subcircular structures on digital images has already given rise to a great deal of research. Different versions of the Hough transform [1] where proposed and applied to various fields in order to detect the center and radius of circular structures.

The version defined by Kimme *et al.* [2] and developed by Gerig and Klein [3] was used by Cross [4] among others, for detecting circular geological structures on a MSS Landsat image. More recently, we elaborated on a methodology [5] partly based on a version of the Hough transform [6] and applied it to Spot images.

We observed that the search for the centers and radii by means of the Transform was not sufficient for detecting all the structures contained in a complex image such as a satellite image. Therefore we developed, prior to the use of the Transform, an algorithm that is able to extract subcircular structures, one by one, and to specify downstream the location of the center and radius of each structure. Applying these algorithms requires the prior extraction of the significant contours.

The methodology consists of two major steps: (a) extraction of significant contours, essentially based on the Mathematical Morphology in the previous paper [5], and on a smoothing followed by an automatic thresholding as described in the present paper; (b) detection of subcircular structures from the significant contours. A contour following operation [7], [8] is generally used to obtain a set of points that lie on the boundaries of the studied regions. Here, contour following is used to individualize the significant contours and split them into a set of subcircular elements when the contours present a change in the direction of curvature.

For each subcircular element, a reference circle (RC) is computed using the result provided by the Hough Transform. The reference circle (RC) is the one whose pixels intersect the maximum number of the contour pixels. This procedure partly differs from curve-fitting techniques [8] that approximate the contour by pieces of smoothed curves.

In addition, our goal of shape recognition requires more than the mere notion of center and radius to characterize structures. These features may be either closed or open, circle arcs of a length smaller, equal to, or greater than that of a semicircle, more or less regular shapes of various orientation, etc.

With this aim in view, new parameters have been defined in this paper for the discrimination of the detected structures. They are: the location of the center and the radius of the reference circle, the number of pixels in the detected contour, the intersection coefficient, the chord coefficient, the direction of the normal to the chord, and the coefficient of symmetry. These parameters are defined and detailed in Section IV. The analysis of this set of data allows us to distinguish and select the various families of desired structures; it is also possible to define these various families by a statistical analysis.

Note that to refine the extraction and individualization of subcircular structures, we have added the notion of "probable inflexion point" (PIP), which was not considered in the method described in our preceding paper [5]. This notion is detailed in Section III.B.

To illustrate our method, we used a Spot subscene from the region of Azru located in the Maroccan Middle Atlas (Fig. 1(a)). We will analyze the parameters and their combination, and the nature of information provided by the method for different families of circular or subcircular structures. The

Manuscript received December 17, 1990; revised September 13, 1991; rerevised February 12, 1992.

J.-F. Parrot is with the Department de Géotectonique, Université Paris VI, 4 place Jussieu 75252 Paris, France, et ORSTOM 70 route d'Aulnay, 93140 Bondy, France.

H. Taud is with the Université Paris VI, et Laboratoire d'Electronique et de Traitement du Signal, Université Mohammed V, rue Ibn Battouta, Rabat-Agdal, Maroc.

IEEE Log Number 9200746.

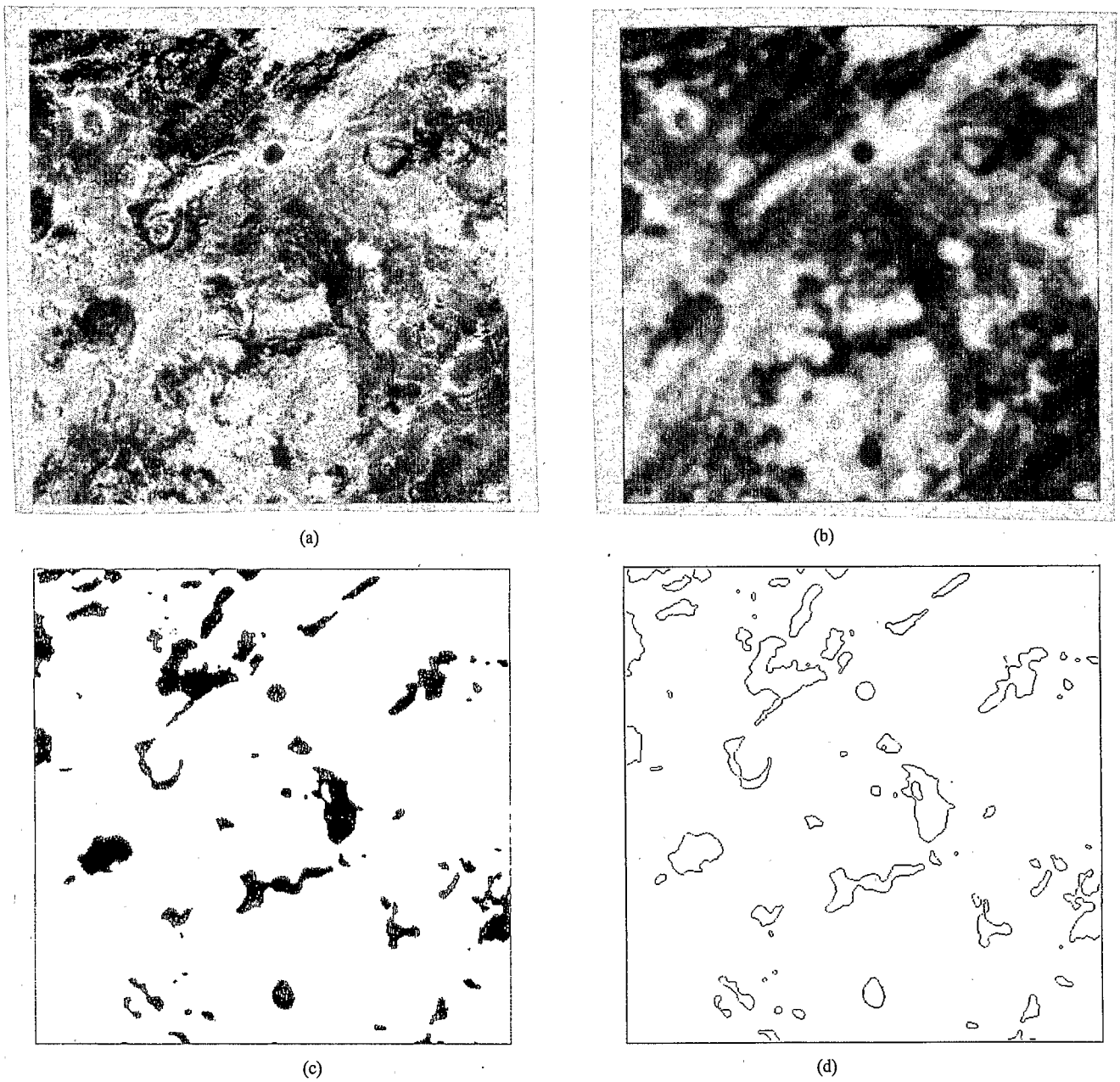

Fig. 1. (a) Thresholding of the XS3 channel of the scene under study (Azru region). (b) Iterative smoothing of the same scene. (c) Binary image obtained by a threshold of value N. The pixels whose values are lower than or equal to n corresponds to 10% of the total number of pixels contained in the image, are recorded with value 1 (in black on the bilevel image). (d) Limits obtained for the image in (c).

results are compared with the geological data in order to improve the methodology.

II. Extraction of Significant Contours

The extraction of the structural elements contained in a satellite image highly depends on their texture. In the given example, the researched structures mainly correspond to the limits of more or less homogeneous reflectance areas, and not to linear features such as a network of roads which would appear as regions that are only a few pixels wide.

In order to smooth the details and reduce the grey level range, an iterative 3×3 low-pass filtering is applied to the raw data image. Iteration stops when the number of pixels modified in the course of the last iteration is smaller than or equal to 1% of the number of pixels modified at the very first filtering (Fig. 1(b)).

The values of the smoothed image histogram are thresholded from a variable reflectance threshold of value N, such that the number of pixels whose values are lower than or equal to the threshold corresponds to a given percentage of the total number of pixels contained in the image. Here, nine levels of percentage were set, every 10%, from 10% to 90%. In each of the scenes thus obtained, the pixels of the smoothed image that correspond to the pixels whose reflectance is lower than or equal to the threshold N, are coded with value 1 whereas the background is coded 0.

The individualization and the detection of subcircular elements as described in Section III, impose the following conditions on the contours:

```
IM is the image to be traced, i corresponds to the lines and j to the columns
for j = 1, number_of_column
  for i = 1, number_of_line — 1
      Dif = IM(i,j) — IM(i+1,j)
       if position equal to 'max_value' then                condition (a)
              if Dif > 0 then RI(i,j) = |Dif|, when RI(i,j) ≤ |Dif|
              else                RI(i+1,j) = |Dif|, when
                                  RI(i+1,j) ≤ |Dif|
       endif
       if position equal to 'min_value' then                        condition (b)
              if Dif > 0 then RI(i+1,j) = |Dif|, when RI(i+1,j) ≤ |Dif|
              else                RI(i,j) = |Dif|, when RI(i,j) ≤ |Dif|
          endif
       end
end
```

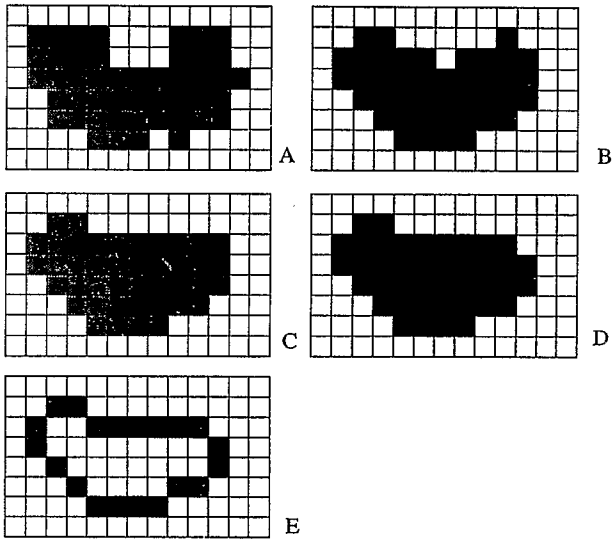

Fig. 2. Illustration of the iterative majority filter and limit tracing.

a. The contour must present an 8-connectivity: the vertical or horizontal straight segments of 1 to n pixels which compose the curve are linked only by their corners.
b. The difference between two successive chain-codes describing the curve must be equal to 0 or ±1.

This type of contour is obtained using the following treatments:

Each of the nine binary images is applied a 3×3 majority filter [9]. This smoothing is iterated until there is no pixel modified by the filtering (Fig. 1(c)). On binary images, the 3x3 majority filter has the advantage of clipping the shapes and of suppressing right angle pixels (Fig. 2). The 3×3 majority filter is quite comparable to Mathematical Morphology operators in that it smooths the shapes. But classical Mathematical Morphology operators such as erosion, dilation, closing, or opening [10], [11] were not used, because the contours obtained by the further algorithm from the smoothed shapes do not entirely satisfy the constraints formerly defined.

Finally, the limits of the resulting shapes are traced by analyzing the skips of values between two neighboring pixels, according to two directions (NS and EW). The algorithm developed is general and can be applied either to a binary image or a multilevel image. Moreover, the limit of the shape can be traced either all around the shape or on the border itself. The Resulting Image (RI) where the contours will be reported is initialized at zero. The steps of the algorithm for the NS direction are listed at the top of the page:

Position is defined at the beginning of the procedure, according to the information researched. Applying condition (a), the absolute value of the difference between reflectance values of two neighboring pixels (i,j) and $(i+1,j)$ of the image IM is reported on the plane RI at the position corresponding to the maximum value encountered in the pair $(i,j)(i+1,j)$. Applying condition (b), the absolute value of the difference is reported at the position corresponding to the minimum value.

A similar process is applied according to the WE direction, taking into account the values previously obtained on the plane RI. Each line i of the traited image IM is scanned from left to right.

In the general algorithm, the NS and WE treatment is followed by a scanning from the NW to the SE and by an other one from the NE to the SW. The contour obtained in this case closely corresponds to borders provided by classical treatment of contour following.

The condition (a) is applied on the nine binary images for the two directions, from N to S and from W to E, in order to obtain an 8-connected contour corresponding to the border of the shape itself (Figs. 1(d) and 2(e)).

All the structural features (secant or isolated, straight lines or curves) revealed through the process of contour extraction are next subjected to detection and individualization treatments.

III. Detection and Individualization of the Subcircular Elements

The four steps of the processing involved by the detection and individualization of the subcircular elements are applied to the contours previously defined.

A. Individualization of the Contours

The curves are individualized one by one through a contour-

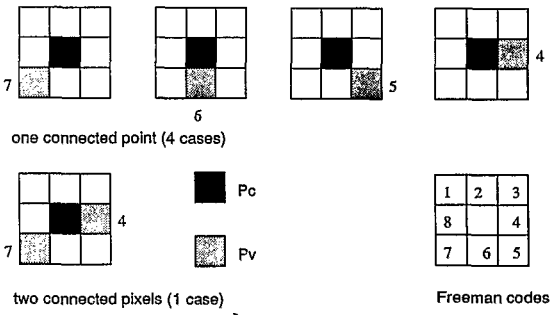

Fig. 3. Freeman code and possible configurations of pixels found in the window W_1.

following procedure that is based on the movement of a sliding 3×3 pixel window W_n; the index n indicates the position of the window on the nth pixel of the contour. The algorithm [5], [12] allows one to decide which direction to follow and whether or not a crossing occurs.

(1) contour following

The contour-following operations are based on the Freeman code [13]. The contour following technique takes into account contours that are either closed or open. When the contour is open, it has two "ends of branch"; by this we mean the absence of pixel connected to the central pixel of the last tested window.

The developed method is the following:

Let Pc be the central pixel of a window W_n and Pv_k be the pixel connected to the central pixel of the same window; where $k = 1, \ldots, K$ and K corresponds to the number of connected pixels.

The whole image is scanned line by line, from left to right. When a contour pixel is hit, the 3×3 window (W_1) centered on the pixel (Pc) is tested.

Owing to the iterative 3×3 majority filtering applied on the binary image, only five configurations may be found in the window W_1 (Fig. 3). The position of the connected pixels is recoded according to the chain-code reported in the Fig. 3.

(a) Only one pixel P_{v_1} connected to the central pixel (P_c); the code of P_{v_1} (code 4, 5, 6 or 7), indicates which direction to follow.

(b) Two pixels (P_{v_1} and P_{v_2}) connected to the central pixel (P_c). One of the connected pixel (P_{v_1}) is always located in the SW corner (code 7), the second (P_{v_2}) is on the right of P_c (E direction, code 4). The first move of the window is always directed toward the SW (code 7) and the code of the second direction (code 4) is stored in memory, to be taken into account if the first chosen direction reaches an end of branch.

When only one connected pixel is observed, this means that we reach one of the extremities of an open contour. If two connected pixels are found, this implies that we have reached a contour, either closed or open, in any of its points. In the second case (two connected pixels P_{v_1} and P_{v_2}), when the contour is open, the sliding window follows the contour to the end of the first branch, and then returns to W_1 to follow the second branch. When the contour is closed, the sliding window goes back to the starting point (W_1) without interruption.

In all cases, the movement of the window from a point n to a point $n+1$ suppresses the central pixel P_c, so that they are not taken into account in the next window.

(2) crossings

When going from position W_n to position W_{n+1}, the code of the direction chosen in W_n is stored in memory so as to be matched, whenever necessary, with the code determined by P_{v_k} in W_{n+1}. In case there exists only one connected pixel, we keep on following the contour whatever the direction may be. On the other hand, if there exists more than one connected pixel, we are either in the presence of a junction point of three branches (two pixels), or of a crossing (three pixels). The choice of the direction to follow depends on the preceding code and on a series of conditions that may be summed up as follows:

Let C_n be the chain-code encountered in the window W_n and C_{n+1} the chain-code of the window W_{n+1},

—condition 1: $| C_n - C_{n+1} | \leq 1$; the absolute value of the difference between the two codes must not exceed 1.

—condition 2: $| C_n - C_{n+1} | = 0$; the first condition may not be sufficient, if it is satisfied by two or three connected pixels; then the selected pixel must also meet condition 2.

—condition 3: when two connected pixels satisfy condition 1 and none of them satisfy condition 2, in other words, when the two possible directions are situated symmetrically on either side of the direction selected in W_n, a test is performed which comes into a general rule corresponding to condition 3.

For each of the possible directions (A and B) found in the window W_{n+1} the value M is computed

$$M = \left| \sum_{j=0,i-1} C_{(n-j)} - \sum_{j=1,i} C_{(n+j)} \right| .$$

The value i corresponds to the number of codes to be considered to decide a direction.

The selected direction is the one whose value M is the lowest (Fig. 4).

$$M_A - M_B \neq 0 \Rightarrow D = A, \text{ if } M_A < M_B$$
$$D = B, \text{ if } M_A > M_B$$

where D is the selected direction.

As long as $M_A - M_B = 0$, the value of i increases until one reaches another crossing, the end of a branch, or else when $i = n$. If condition 3 cannot be satisfied within these limits, then the crossing found in W_{n+1} is considered an end of branch. At the end of contour detection, the crossing pixels, if any, are reactivated so as to be ensure continuity of the contours not yet detected.

B. Decomposition of the Curves into Subcircular Elements

The contours individualized in the previous step are sometimes formed by a succession of subcircular elements which are alternately convex and concave. The contour is segmented into subcircular elements when a change in the curvature direction occurs.

In the discrete mode a curve can be decomposed into a succession of straight lines consisting of one to n pixels and whose directions are either vertical or horizontal. Owing to the iterative majority smoothing applied to binary image, the shape-border curves obtained by the algorithm described in

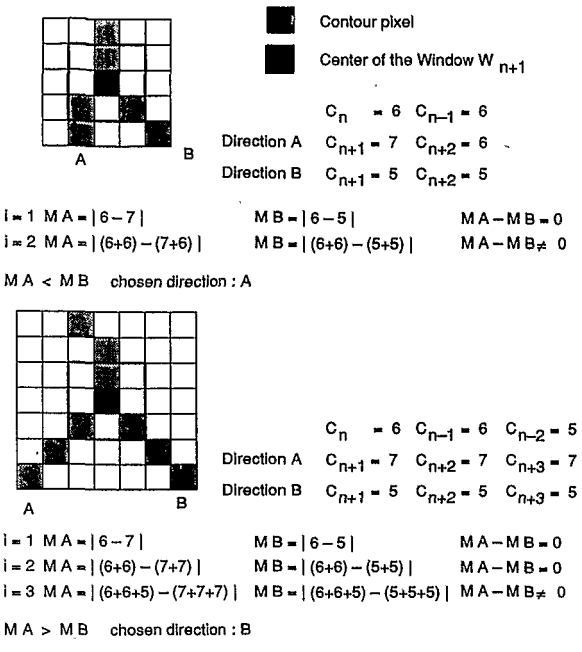

Fig. 4. Two examples of the application of condition 3. (crossings).

Section II correspond to curves in 8-connectivity (Fig. 2). Thus, the difference between two subsequent values of the chain-code is equal to 1, 0 or −1. If we do not take the value 0 into account, we observe a regular alternation of 1 and −1 values. This pair of values (1/−1 or −1/1) marks the passage between two subsequent straight line segments of the curve, and remains identical as long as the segments keep the same direction (horizontal or vertical), or as long as the move along the perpendicular axis with respect to the direction of these segments does not change. A change is expressed by the inversion between the value of the pair, the pixel $P(i, j)$ where this inversion occurs is defined as a "critical point" [5], [12]. This definition is more restrictive than the one proposed by Hung and Kasvand [14] who consider any pixel where the difference of code is not nul as a critical point, which requires a series of additional tests to know whether we are in the presence of a true change of direction or not.

In order to find where a change in the curvature direction occurs, the shape of the curve must be examined at each critical point. This examination takes place in a window of increasing size centered on the critical point. The window is divided into two equal parts by a straight line (separating line) which passes through the critical point and the center of the window and which contains the maximum number of contour pixels found in one of the following four directions: NS, EW, NESW, or NWSE.

The window increases until there is no contour pixel left on the two end pixels of the separating line. At this stage, the pixels of the considered contour which are not on the separating line are located either on both sides of this line or one side only.

The first location implies a change of curvature directly noticeable on the window. The second one allows to code the curvature direction: the code 1 is retained when the contour pixels out of the separating line are only located

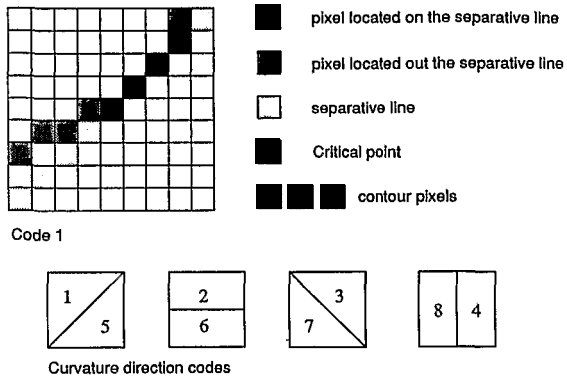

Fig. 5. Codes of curvature direction.

northwestwards, the code 2 is applied for a northern location, the code 3 for a NE location, etc . . . (Fig. 5); in the example given in the Fig. 5, the pixels which are not on the separating line are located in the NW and the curvature direction is equal to 1. There is a change in curvature when the contour pixels are distributed on both sides of the separating line, or when the absolute value of the difference between to successive codes of curvature exceeds 1.

It should be noted that there exists a kind of inflexion point which does not present the characteristics of a critical point as formerly defined and that was not considered in our preceding paper [5]. As a matter of fact, it is a change of direction without any inversion of the pairs and with the same perpendicular displacement, as the successive straight line segments keep the same direction. We can only observe that the number of pixels comprising the successive segments increase more or less regularly. Their numbers increase and then decrease (Fig. 6), or vice-versa. When an increasing is followed by a decreasing, the last pixel of the greater straight segment is considered as a point candidate to be an inflexion point. It is denoted "Probable Inflexion Point" or PIP. When a decreasing is followed by an increasing, PIP is the last pixel of the smaller straight segment.

If the absolute value of the difference between the curvature codes of two successive critical points equals 4, the PIP is considered to be a real inflexion point corresponding to the middle of a S-contour and the curve is split on the PIP. This procedure has the advantage of cutting the curve only if confirmation of a change in the curvature direction is recorded (Fig. 6). Thus, shapes of more or less regular contours are entirely taken into account.

C. Application of the Hough Transform

When a subcircular element is individualized by the preceding substep, a version of the Hough Transform [6] is then applied in order to determine the approximate location of the center of this element and the approximate value of its radius.

The Hough Transform [1] converts a complex problem of shape detection in image space into a peak detection problem which is easier to solve in parameter space. The latter is quantized and used as an accumulator. The Hough Transform was generalized and specialized to solve various problems in

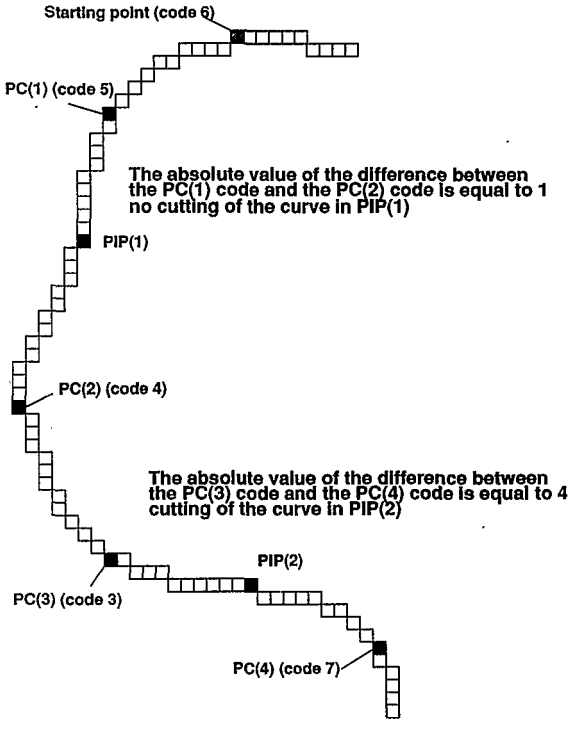

Fig. 6. Probable Inflexion Point and decision for splitting.

many fields, in particular for detecting circular structures [2], [15]–[19].

Illingworth and Kittler [6] used a two-dimensional parameterization to determine the position of the center, followed by one-dimensional parameterization to find the value of the radius. The detection of a circle depends on the following constraint: all the vectors normal to the tangent at each point of the contour must intersect at only one point, which corresponds to the center of the circle. The estimation of the normal directions may be obtained by local contour detection operators such as the Sobel.

D. Finding the Exact Location of the Center

With the Hough method, the detection of circular structures is essentially based on the contour pixels. Another approach consists of considering all the pixels which do not belong to the contour as probable centers of this contour. Thus, for each probable center, the distance d of the center to the contour pixels can be computed from:

$$d = \left[(x_i - x_p)^2 + (y_i - y_p)^2\right]^{1/2} \tag{3}$$

where x_i, y_i represent the coordinates of a contour point and x_p, y_p the coordinates of a probable center; $i = 1, \ldots, I; p = 1, \ldots, P$; I: number of contour pixels; P: number of pixels which do not belong to the contour.

Thus, for each probable center, we obtain a histogram containing, on the x-axis, the values of the distances and, on the y-axis, the frequency of these distances. The maximum $\mathrm{Max_p}$ found on the histogram corresponds to the most frequent distance between the probable center and the pixels of considered contour. The distance d_p is then considered as the radius value of a given center.

The maximum $\mathrm{Max_p}$ together with the value of the corresponding distance d_p are recorded in the tables $M(x_p, y_p) = Max_p$ and $R(x_p, y_p) = d_p$. Thus, when all the probable centers have been tested, the maximum found in the table $M(x_p, y_p)$ allows one to find the exact location of the required center. The correspondence established between $M(x_p, y_p)$ and $R(x_p, y_p)$ provides the value of the radius.

To improve the efficiency of the search for the circle center, a limited search area is an area that surrounds the highest values found in the accumulator. The selected area is a window whose size is determined by the uncertainty value computed at the previous step, and it is centered on the approximate center resulting from the application of the Hough Transform.

The circle thus detected, which we call Reference Circle (RC) and which satisfies the experimental requirements (for example, a contour of 50 pixels at least, a segment of 50 pixels at least, an intersection of more than 20%, etc . . .), corresponds to the circle that includes the maximum number of pixels of the considered contour. It may contain all the contour pixels or inscribe or be inscribed in it.

IV. Characteristic Elements of the Detected Structures

When the exact position of the center (x, y) and the precise value of the radius (R) of the Reference Circle (RC) are known, the algorithm provides for each detected subcircular element the center coordinates and the radius value of the circle, along with additional information allowing a better individualization of the detected structure.

All these parameters are recorded in a table which indicates respectively: the number of the detected structure, the x and y positions of the center of the reference Circle (RC), the value of the radius (R) of this circle, the number of pixels in the detected contour, the intersection coefficient, the chord coefficient, the direction of the normal to the chord and the coefficient of symmetry, the occurrence (OCC), the position x, y of the chord beginning, the position x, y of the chord end, and a series of ordering numbers depending on the occurrence (OCC).

Thus, we obtain a table for each of the nine images created by the thresholding described earlier (see Section II). These nine tables are grouped into one of the same type (Table I), which contains all the data related to all the detected structures. Simultaneously, in order to reduce the data requirement, only the coordinates of the sequence of pixels forming the detected contours for each of the nine images are stored. The resulting data consists of a set of l_i elements

$$L = \{l_i \ : \ i = 1, \ldots, n\}$$

where l_i represents the set of the points of the detected contour.

$$l = \{P_j = (x_j, y_j), j = 1, \ldots, m\}.$$

TABLE I

	x	y	R	npdc	IC	DIR	CC	DNC	OCC	extremities of the chord				
1	41	215	22	70	32	303	31	73	1	77	181	27	214	1
2	45	66	9	52	26	338	63	78	1	58	40	42	80	2
3	123	158	26	58	31	277	19	35	1	140	141	84	148	3
4	145	155	11	51	38	67	95	9	1	140	141	161	150	4
5	221	136	20	98	34	197	95	45	1	209	156	194	108	5
6	207	132	25	56	51	177	46	24	1	211	120	209	156	6
7	351	224	22	77	22	164	8	95	1	370	216	351	282	7
8	461	269	14	79	36	1000	100	0	1	465	256	465	256	8
9	45	336	8	62	25	320	42	238	1	49	329	6	380	9
10	136	260	11	61	71	1000	100	0	1	125	260	125	259	10
11	209	151	28	50	41	275	23	4	1	230	133	183	137	11
12	204	148	38	56	35	220	13	3	1	240	148	209	111	12
13	221	163	17	51	42	140	23	29	1	230	168	220	180	13
14	201	285	17	63	31	23	137	35	1	198	270	215	311	14
15	189	287	17	52	28	223	4	41	1	220	294	198	270	15
–	–	–												
–	–	–												
–	–	–												
108	395	180	9	52	42	1000	100	0	1	399	175	399	175	108
109	491	304	16	76	32	1000	100	0	1	480	309	480	308	109

A. Definition of the Parameters

(a) n_{pdc}: number of pixels of the detected contour.

(b) IC: intersection coefficient. It is the percentage of the RC pixels that intersect (n_{pi}) the pixels of the considered contour (n_{pdc}); $IC = (n_{pi}/n_{pdc})*100$. In the designed algorithm, the contour is taken into account only for a IC greater than or equal to 20. The higher this coefficient, the closer the contour to a circle or to a circle section.

(c) DIR: direction of the normal to the chord of the detected element. The normal to the chord passes through the center (x, y) of RC. The values are expressed in degrees and are coded clockwise, the origin (0°) is situated to the north of the image. For a satellite image, note that the real geographical direction corresponds to this value plus the angle of the satellite trajectory.

(d) CC: chord coefficient. $CC = (\ln/2R)*100$, ln is equal to the distance between the intersection of the normal to the chord and the intersection of the normal with the contour. This coefficient allows one to figure the shape of the contour concerned. A coefficient lower than 50 corresponds to an arc smaller than the semicircle, a coefficient higher than 100 means that the RC circle is inscribed in the detected contour. As a rule, the coefficient of closed structure is set to 100, which corresponds to a complete circle, and whatever the IC of this shape may be.

(e) DNC: is the ratio expressed in percentage of the distance between the intersection of the normal to the chord with the middle of the chord to the radius value (R). Thus, the DNC value that is equal to or close to 0 indicates that the subcircular structure is symmetrical.

Fig. 7 illustrates the definition and the calculation of these parameters.

(f) OCC: is the occurrence, that is, by definition equal to 1 in Table I.

B. Notion of Occurrence

As the processed image has been thresholded into nine images according to the percentage, same subcircular structures may be detected several times. This is due to the following phenomena:

(a) A shape detected for a reflectance threshold depending on the selected segmentation percentage can be preserved, with or without dilation, for the reflectance threshold(s) of other percentage brackets, without being absorbed into a new shape.

(b) Different thresholding levels may reveal different sections of the same structure.

Moreover, the decomposition into subcircular elements performed on the limits of the shapes may split the same circular structure into several circle arcs.

Thus, when the nine images are grouped, we often obtain similar centers and radii for different structural features. At this stage, we want to know the number of structural elements whose center and radius are comprised in a given interval. This number corresponds to the occurrence (OCC). With this occurrence, recoded on Table II, is (are) associated the number(s) of the concerned structures found in Table I.

This allows one, in the course of the later treatments processed from Table II, to look up in Table I the specific characteristics of each structure considered to form only one element in Table II.

In addition, the search for the occurrence in a given interval involves the modification of certain parameters, namely: x, y, R, and DIR. By convention, and to preserve the same layout for the two tables (which allows to proceed directly to the selections from Table I), the other parameters, not used from Table II, are set to zero.

$$x = \sum x_i/occ \ (i = 1, \ldots, occ)$$

$$y = \sum y_i/occ \ (i = 1, \ldots, occ)$$

$$r = \sum r_i/occ \ (i = 1, \ldots, occ)$$

$$\begin{aligned} dir_{occ} &= (dir_i + dir_{i+1})/2 && \text{if } |dir_{i+1} - dir_i| < \\ &= (dir_i + dir_{i+1})/2 - 180^\circ && \text{if } |dir_{i+1} - dir_i| > 18 \\ &= 2000 \text{ by convention,} && \text{if } |dir_{i+1} - dir_i| = \\ & \quad i = 1, \ldots, occ - 1. \end{aligned}$$

By convention, if one of the encountered directions is equal to 2000 (corresponding to a closed structure), the resulting direction (dir_{occ}) is set to the same value. Besides, if the two directions are opposed the dir_{occ} value recoded in Table II is 3000, since the structure is considered a circle formed of discontinuous segments.

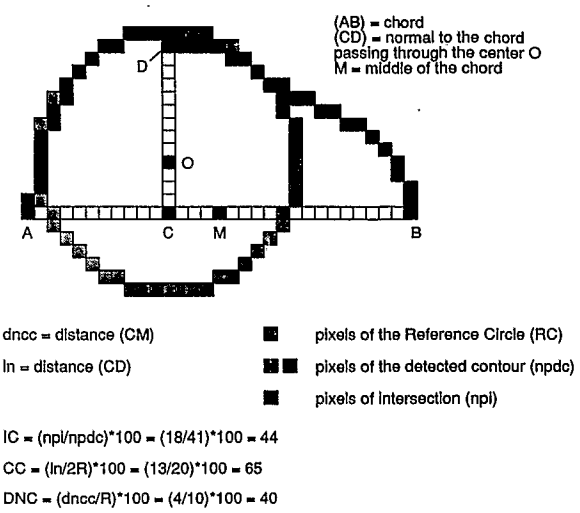

Fig. 7. Example of the computing of the discriminant parameters.

TABLE II

	x	y	R	npdc	IC	DIR	CC	DNC	OCC	extremities of the chord	ordering numbers
1	460	271	18	–	–	1000	–	–	2	– – – –	8 71
2	136	260	12	–	–	1000	–	–	5	– – – –	10 28 38 52 62
3	209	151	32	–	–	210	–	–	3	– – – –	11 12 24
4	310	86	24	–	–	74	–	–	4	– – – –	18 30 43 67
5	352	206	19	–	–	64	–	–	6	– – – –	19 41 50 64 79 96
6	463	249	30	–	–	189	–	–	3	– – – –	22 33 45
7	19	24	32	–	–	90	–	–	2	– – – –	26 36
8	174	481	21	–	–	190	–	–	2	– – – –	29 39
9	304	309	14	–	–	63	–	–	4	– – – –	40 55 81 93
10	323	386	25	–	–	252	–	–	6	– – – –	42 54 66 82 94 104
11	95	69	29	–	–	149	–	–	2	– – – –	48 61
12	389	157	30	–	–	291	–	–	2	– – – –	51 65
13	–6	317	33	–	–	153	–	–	2	– – – –	58 72
14	58	464	31	–	–	169	–	–	3	– – – –	60 73 88
15	416	390	18	–	–	176	–	–	2	– – – –	70 86
16	189	57	32	–	–	303	–	–	2	– – – –	77 92
17	358	53	15	–	–	329	–	–	3	– – – –	80 97 106

V. Results and Analysis

The treatment was performed on the XS3 band of a 512×512 pixel subscene (lines: 1220–1731; columns: 2430–2941) of a Spot image acquired on April 30, 1986 (reference WRS 35–283; level: 1B; incidence: 2.4; azimuth: 130; elevation: 66). The region of Azru (Maroccan Middle Atlas), covered by this subscene, includes numerous subcircular structures of volcanic and karstic origin. The plateau of Azru, bounded northwards by the monoclinal series of Bou-Terrouine located in the upper part of the subscene, is mainly composed by volcanic rocks of ante-Würm age, lying on a karstic, liasic basement which reappears locally [20]. Regular cones and explosive craters are scattered onto the plateau. Volcanic cones are covered by cedar woods, as the vegetation of whole plateau corresponds to a steppe with ligneous chamephytes [21]. The results are the following: 109 subcircular detected structures, considering the threshold set to take them into account (Fig. 8(a)). These thresholds concern the minimum number of pixels forming a contour (50 pixels), on the one hand, and the intersection coefficient IC, that must be equal to or greater than 20%, on the other hand. The deliberately low value of the IC produces a great variability of the detected shapes, the analysis of the characteristic parameters will enable to sort them.

The rather high number of the detected structures is partly due to the successive processing of the nine images generated by the thresholding by percentage bracket.

The characteristics of these 109 "primary" structures are recorded in Table I. As mentioned above, the structures whose centers and radii are equivalent or similar, can be grouped (Fig. 8(b)) into one element in Table II, where we list the occurrence (that is, the number of structures composing this element) and the ordering numbers of these structures as recorded in Table I. This allows one to look up in Table I the characteristics of these structures and in the set of the pixel-coordinates L, so as to be able to trace the structures whenever necessary, as well as the chord and normal to the chord.

The parameters characterizing the detected structures and/or their combination allow one to discriminate between the encountered shapes.

Thus, a closed contour, whose CC is by definition equal to 100, is regular when the IC is high, and irregular when the IC is low. An elliptic section may have a low IC and a low CC, or an average IC and a CC higher than 100. A semicircle arc has a CC close to 50. A CC higher than 100 indicates that the RC is inscribed in the detected contour. The symmetry of these shapes are inversly proportional to the DNC. In addition, the subrectilinear structures are characterized by a low IC and a low CC.

In this way, a user can base his choice on his own thematic concerns, for example, on the search for circular arcs whose normal to chord is comprised in a given interval. In the case of this particular choice, illustrated with Fig. 8(c), the detected circular arcs are regular (IC comprised between 33 and 100), and are greater or slightly smaller than the semicircle, notwithstanding the closed shapes (CC comprised between 33 and 99). Moreover, they are symmetrical to subsymmetrical (DNC comprised between 0 and 50).

According to our objective of the automatic detection of structural features, the sorting out of the structures may be done by means of a statistical analysis whose results do not contradict the user's choice; even better, they allow him to control his choice and test the real weight of the parameters in the class partition.

Without going into too much detail, we observe for the set of the 109 "primary" structures, that:

- — 40% of the radii are between 15 and 22, that is 300 to 440 m,
- — 85% of the IC are between 20 and 50.
- — the directions (DIR) are isotropic,
- — according to the CC, 49% of the arcs are smaller than semicircles,
- — 19% are close to being semicircles and 12% correspond to closed structures.
- — 48% of the structures have a DNC smaller than 20, which means they are subsymmetrical.

The total or partial correlation matrix shows that all these parameters are highly uncorrelated, which makes all the more relevant the hierarchical analysis on which is based the grouping of the structures into different classes.

Since this illustration of our results did not aim at discriminating between the structures according to the direction of the normal to the chord and to the radius value, the only

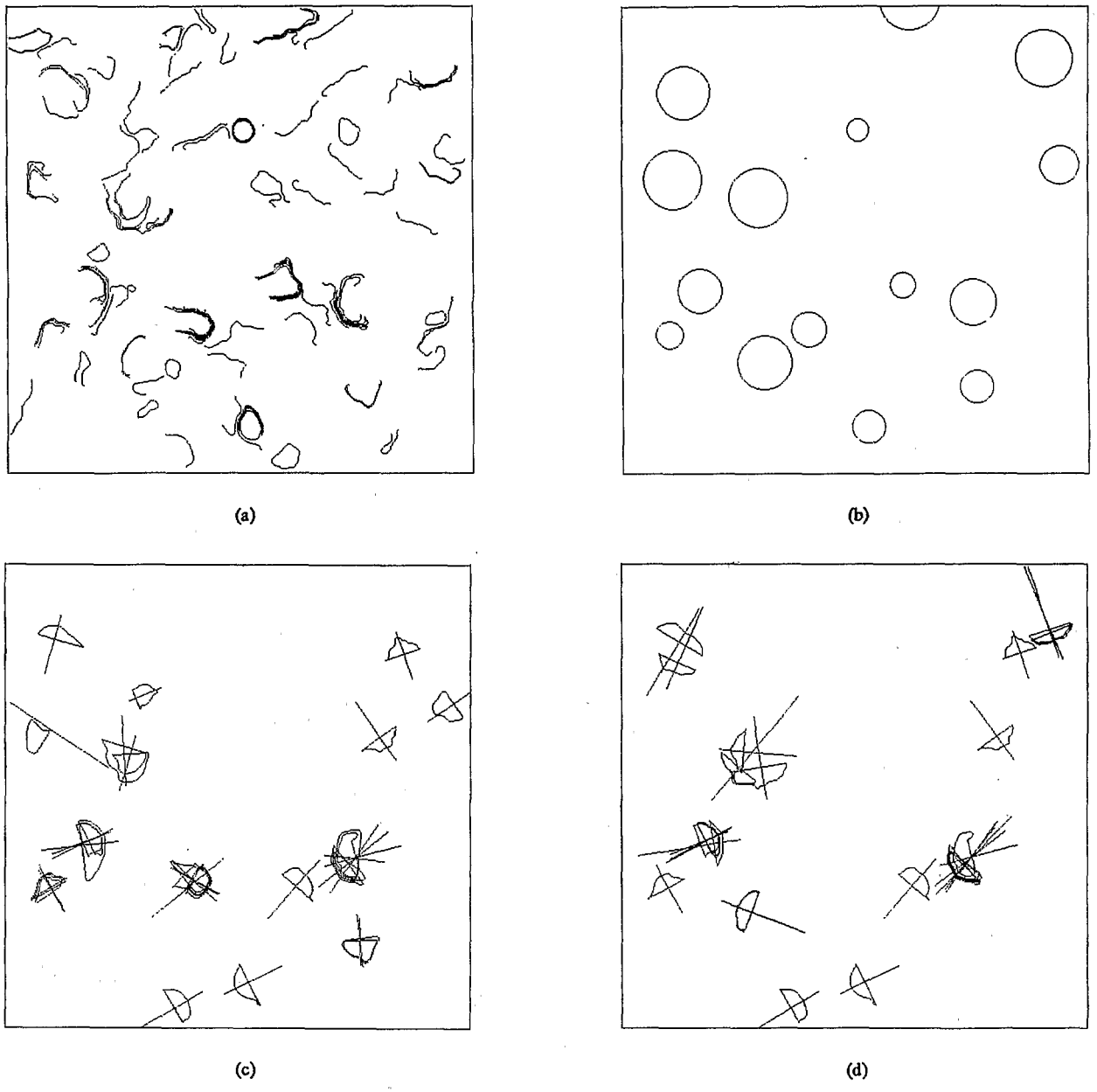

Fig. 8. (a) Set of the structures detected in the Azru region. (b) Detected structures for an occurrence greater than or equal to 2 (see Table II). (c) Examples of a user's selection (IC: 33–100; CC: 33–99; DNC: 0–50). (d) Classe 16 obtained by statistical analysis (IC: 32–70; CC: 13–48; DNC: 0–14).

discriminating parameters we retained are the following: IC, CC, and DNC, in order to perform the ascending hierarchical analysis taking the Euclidean distance and the mean value of the weighted distances as aggregating criteria [22].

By restricting the segmentation of the hierarchical tree to less than 25 individuals for the class which contains the maximum number, we obtain 16 classes presented in Table III.

As an example, the 24 structures forming the class 16 were put in Fig. 8(d), by taking the minimum and the maximum of the discriminating parameters IC, CC, and DNC. In this case the identified objects do not come from a subjective choice, but directly result from the classification. They are not significantly different from those of Fig. 8(c), as the statistical treatment limits more precisely the discriminating parameters on more objective criteria.

Apart from all thematic concerns, we tried in this paper to discriminate between the detected structures only from their shapes. Comparing our results with the ground data [20], one can notice that the detected structures mainly correspond to geological structures (limits of formations, circular structures produced by volcanic and/or karstic activity, following of lithological layers, etc . . .). A study is under way to find more information about the nature of each geological structure, and to allow their discrimination. It is mainly based on the statistical analysis of the data such as the vegetation cover [21] contained in the surfaces described by the circles or circle arcs and associated chord. The individualization of structural families is then based not only on the parameters described above (R, IC, CC, DNC, and DIR), but also on the parameters given by the reflectance values of the different Spot channels, and by the application of a specific index

TABLE III

Classe	Individuals Number	IC (aver,min,max)	CC (aver,min,max)	DNC (aver,min,max)
1	12	30,21,45	2000,2000,2000	2000,2000,2000
2	1	25,25,25	42,42,42	238,238,238
3	1	25,25,25	100,100,100	333,333,333
4	15	26,20,36	16,0,43	69,41,95
5	1	29,29,29	50,50,50	144,144,144
6	4	28,26,32	122,100,138	82,64,89
7	1	30,30,30	250,250,250	33,33,33
8	1	31,31,31	200,200,200	44,44,44
9	1	26,26,26	63,63,63	78,78,78
10	3	31,24,34	84,64,95	41,33,46
11	14	47,32,71	99,91,100	2,0,13
12	7	42,34,55	53,21,65	9,3,17
13	2	34,32,35	133,131,135	0,0,0
14	1	31,31,31	137,137,137	35,35,35
15	21	36,22,52	33,13,47	30,12,50
16	24	49,32,70	30,13,48	6,0,14

(vegetation index, brightness index, etc . . .), or else by the values obtained on the derived characteristics resulting from a Digital Elevation Model (slope variation, morphological codes, etc . . .), or even by digitized data such as geological, pedological, or other data.

VI. Conclusion

This paper demonstrates that it is possible to perform the unsupervised detection of subcircular structures from a satellite image, and to classify these structures by means of the discriminating parameters that we have defined. The detection is based on the extraction of the contours from the processed image, and the search for the centers and radii of the subcircular structures contained in these contours.

With each detected structure are associated the discriminating parameters descriptive of the shape. These parameters allow one to sort out the desired shapes, either by defining the limits of these parameters or by grouping these structures into classes by means of a statistical analysis. This method of Automatic Detection Of Numerical Image Structures (ADONIS), which aims at recognizing shapes, not only allows one to detect curves of subcircular shape, but also subrectilinear curves. The sorting, automatic or not, of the shapes is based on the analysis of the discriminating parameters.

Acknowledgment

The authors gratefully acknowledge the reviewers for their helpful criticism and suggestions.

References

[1] P. V. C. Hough, "A method and means for recognizing complex patterns," U.S. Patent 3, 069, 654, 1962.
[2] C. Kimme, D. Ballard, and J. Sklansky, "Finding circles by an array of accumulator," *Commun. Ass. Comput. Mach.*, vol. 18, no. 2, pp. 120–122, 1975.
[3] G. Gerig and F. Klein, "Fast contour identification through efficient Hough Transform and simplified interpretation strategy," 8th Intern. Joint Conf. on Pattern Recognition, Paris, pp. 498–500, 1986.
[4] A. M. Cross, "Detection of circular geological features using the Hough Transform," *Int. J. Remote Sensing*, vol. 9, no. 9, pp. 1519–1528, 1988.
[5] H. Taud and J.-F. Parrot, "Detection of circular structures on satellite images," *Int. J. Remote Sensing*, vol. 13, no. 2, pp. 319–335, 1992.
[6] J. Illingworth and J. Kittler, "The adaptive Hough Transform;" *IEEE Trans. Pattern Anal. Machine Intel.*, vol. 9, no. 5, pp. 690–698, 1987.
[7] A. Rosenfeld and C. Kak, *Digital Picture Processing* (2nd ed.). New-York/London: Academic Press, 1982.
[8] T. Pavlidis, *Algorithms for Graphics and Image Processing.* Berlin, Heidelberg, New-York: Springer-Verlag, 1982.
[9] R. A. Schowengerdt, *Techniques for Image Processing and Classification in Remote Sensing.* New-York/London: Academic Press, 1983.
[10] J. Serra, *Image Analysis and Mathematical Morphology.* London/ New-York: Academic Press, 1982–1988 (2 vols.).
[11] M. Coster and J.-L. Chermant, "Précis d'Analyse d'Images," Ed. CNRS, Paris, 1985.
[12] H. Taud, "Détection des structures circulaires sur image numérique: recherche non supervisée des structures géologiques sur image satellitaire," Th. 3ème Cycle, Univ. Mohammed V, Rabat, 137 p., 1989.
[13] H. Freeman and L. S. Davis, "A corner-finding algorithm for chain coded curves," *IEEE Trans. Comput.*, vol. C-26, pp. 297–303, 1977.
[14] S. H. Y. Hung and T. Kasvand, "Critical points on a perfectly 8- or 6-connected thin binary line," *Pattern Recognition*, vol. 16, pp. 297–303, 1983.
[15] R. O. Duda and P. E. Hart, "Use of the Hough Transform to detect lines and curves in pictures," *Commun. Ass. Comput. Mach.*, vol. 15, no. 1, pp. 204–208, 1972.
[16] D. H. Ballard, "Generalizing the Hough Transform to detect arbitrary shapes," *Pattern Recognition*, vol. 13, pp. 111–122, 1981.
[17] D. Casasent and R. Krishnapuram, "Curved object location by Hough Transformations and interventions," *Pattern Recognition*, vol. 20, pp. 267–276, 1987.
[18] D. S. McKenzie and S. R. Protheroe, "Curve description using the inverse Hough transform," *Pattern Recognition*, vol. 23, no. 3/4, pp. 283–290, 1990.
[19] A. Israel, "Algorithm for finding the centre of circular fiducials," *Computer Vision, Graphics, and Image Processing*, vol. 49, pp. 398–406, 1990.
[20] J. Martin, "Le Moyen-Atlas central. Etude géomorphologique," Ed. serv. géol. du Maroc, Notes et Mém., 258bis, 445 p., 5 cartes HT., 1981.
[21] M. Lecompte, "Biogéographie de la montagne marocaine, le Moyen-Atlas central," Ed. CNRS, Mém. et Doc de Géographie, 202 p., 1 carte HT, 1986.
[22] M. Roux, "Algorithmes de classification," Masson Ed. Paris, 1985.

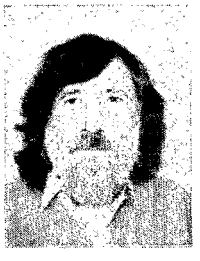

Jean-François Parrot was born in Paris, France. He received the diploma in anthropology and ethnography from the University of Paris in 1966, and in 1967 he obtained the Bachelors degree. He received the Ph.D. degree from the University of Nancy in 1976; it concerned the petrology of mafic-ultramafic assemblages in Greece, Cyprus, Turkey, and Syria.

He spent 12 years as director of the Geological Laboratory of ORSTOM (French Institute of Scientific Researches for the Development in Cooperation) in Bondy (France), and 5 years as director of the ORSTOM Remote Sensing Laboratory. He joined the Remote Sensing and Geotectonic Laboratory of the University of Paris VI in 1986. His present research is mainly in the area of the automated remote sensing image analysis, linear feature detection and classification, pattern recognition, land cover, and land use mapping and monitoring.

Hind Taud was born in Morocco. She received the M.Sc. degree in physics from the University of Fes in 1986 and the B.S. degree in remote sensing from the University of Rabat, in 1989.

Since 1989, she has been a Research Scientist in the Remote Sensing and Geotectonic Laboratory of the University of Paris VI, where she is a Ph.D. candidate. Her research interests are in automated remote sensing analysis, linear feature detection, pattern recognition, and computer vision.